Journal of Applied Polymer Science

# Enhancing compatibility between poly(lactic acid) and thermoplastic starch using admicellar polymerization

**Kasinee Hemvichian,[1] Phiriyatorn Suwanmala,[1] Wararat Kangsumrith,[2] Prapanee Sudcha,[3] Kamonnit Inchoto,[3] Thirawudh Pongprayoon,[3] Olgun Güven[4]**

[1]Nuclear Research and Development Group, Thailand Institute of Nuclear Technology (Public Organization), Ministry of Science and Technology, 9/9, Moo 7, Sai Moon, Ongkharak, Nakorn Nayok 26120, Thailand

[2]Department of Industrial Engineering, Faculty of Engineering, Thammasat University, Khlong Luang, Pathumthani 12120, Thailand

[3]Department of Chemical Engineering, Faculty of Engineering, King Mongkut's University of Technology North Bangkok, 1518, Pracharat 1 Road, Bangsue, Bangkok 10800, Thailand

[4]Polymer Chemistry Division, Department of Chemistry, Hacettepe University, Beytepe, Ankara 06800, Turkey

Correspondence to: K. Hemvichian (E-mail: kasineeh@yahoo.com)

**ABSTRACT:** An alternative method to improve the compatibility between poly(lactic acid) (PLA) and cassava starch (CS) is proposed and investigated. Admicellar polymerization is used to modify the surface of CS with poly(methyl methacrylate) (PMMA) in order to make it more hydrophobic and hence more compatible with PLA. The increased hydrophobicity of PMMA modified cassava starch (MS) is validated by contact angle measurement. Results from iodine test, Fourier transform infrared spectroscopy (FTIR), thermogravimetric analysis (TGA), X-ray photoelectron spectroscopy (XPS), and scanning electron microscopy (SEM) confirm the formation of PMMA film on MS surface. Mechanical properties of PLA-CS and PLA-MS blends are investigated to compare their compatibility. Noticeable improvements in blend tensile strength and elongation at break evidently show that MS is more hydrophobic as well as more compatible with PLA than CS. © 2016 Wiley Periodicals, Inc. J. Appl. Polym. Sci. **2016**, *133*, 43755.

**KEYWORDS:** admicellar polymerization; compatibility; PLA; PMMA; starch; surface

Received 28 October 2015; accepted 8 April 2016

**DOI: 10.1002/app.43755**

## INTRODUCTION

Polylactide or poly(lactic acid) (PLA) is recognized as one of the most promising biodegradable polymers.[1] PLA is synthesized from lactic acid which is derived from renewable resources, thus attracting a great deal of attention as a potential substitute for petrochemical-based, non-biodegradable, synthetic polymers.[2] In addition to biodegradability, PLA offers a number of advantages, from being eco-friendly and non-toxic to having a high melting temperature and being transparent.[3] In spite of these beneficial properties, there are a few factors that prevent PLA from being extensively utilized. In terms of properties, a major drawback of PLA is its low glass transition temperature. In terms of cost, the price of PLA is comparatively higher than other commercial polymers commonly used in packaging materials. Eventually, with constant development, PLA can become a serious contestant for polyethylene (PE), polystyrene (PS) or polyethylene terephthalate (PET). Nonetheless, currently, blending PLA with other polymers, especially natural polymers, has become increasingly attractive, since natural polymers offer a competitive commercial strategy, mainly due to their relatively low cost.

Cassava starch (CS) is a natural polymer that is inexpensive and abundant, especially in Thailand. In addition to being cost-effective, CS is also biodegradable, compostable, nontoxic, and most importantly renewable. Consequently, blending CS with PLA can reduce production cost, while simultaneously preserving biodegradability of their blends. Nevertheless, it is very difficult to process starch because its melting temperature ($T_m$) and decomposition temperature ($T_d$) are very close. Made up of linear amylose and highly branched amylopectin, starch granules contain both amorphous and ordered regions. At temperatures higher than 70 °C, in the presence of a plasticizer such as water,[4] glycerol,[5] or citric acid,[6] the ordered regions, i.e., crystalline structures, of starch can be disrupted. Therefore, the plasticized starch can be thermal processed and is usually named thermoplastic starch (TPS). The fact that TPS can be processed makes it possible to blend PLA and TPS using conventional machines set at temperatures well below the onset of degradation of starch.

However, compatibility between PLA and CS is rather poor, since PLA is hydrophobic while CS is hydrophilic. As a result,

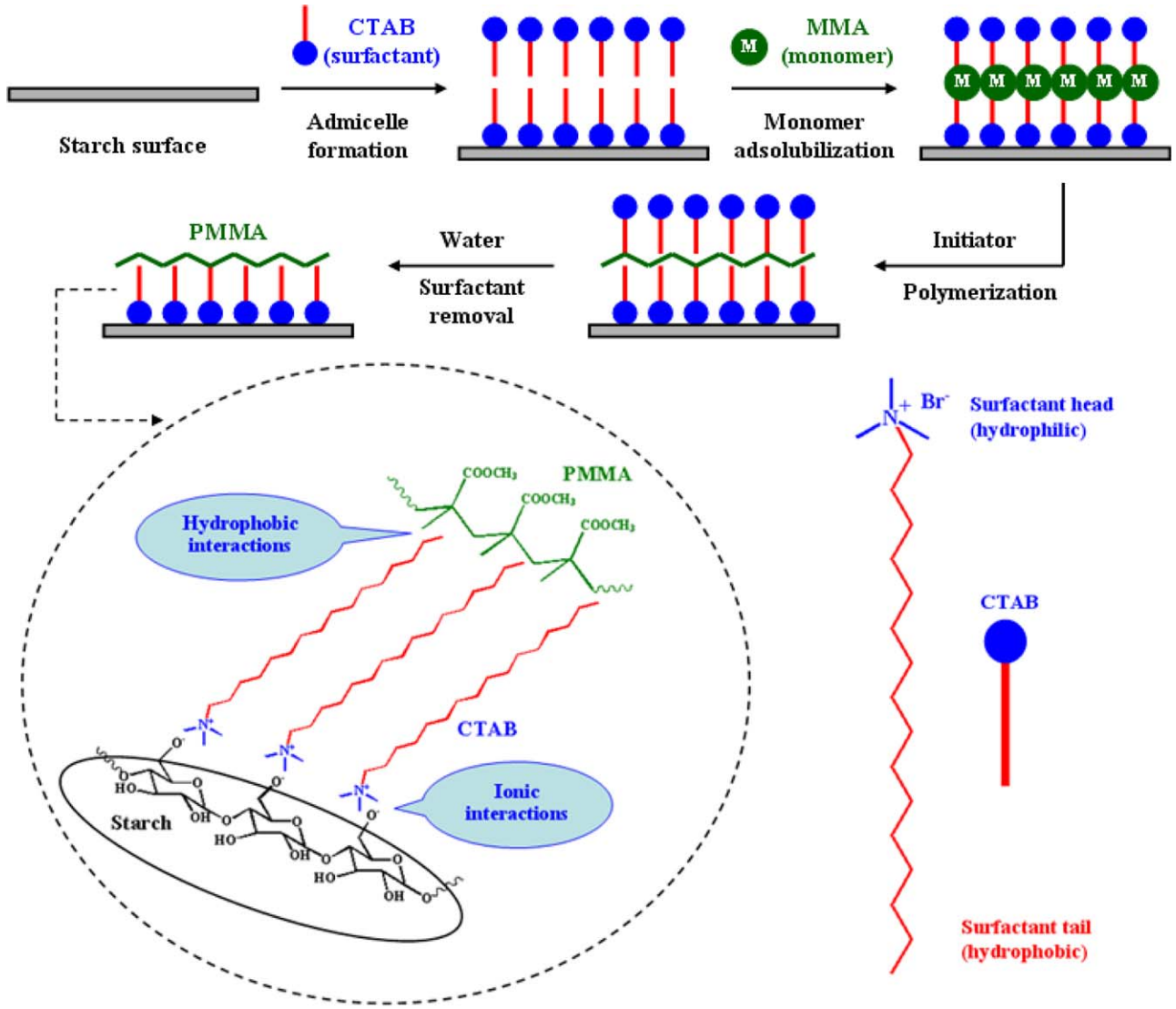


**Scheme 1.** Surface modification of starch by admicellar polymerization. [Color figure can be viewed in the online issue, which is available at wileyonlinelibrary.com.]

they are thermodynamically immiscible.[7] This incompatibility eventually leads to inferior properties of their blends.[8–11] A number of research groups reported their works to improve the compatibility between PLA and starch either by using a compatibilizer,[12,13] by modification of hydroxyl groups in starch[14] or by using coupling agents to modify starch.[15] The use of a compatibilizer or silane coupling agent can offer a reactive blend and large-scale production via continuous extrusion technologies, but machines with special design may be required. Chemical modification of hydroxyl groups in starch is able to provide significant improvements, however sometimes it involves expensive catalyst and large amount of organic solvents. Among these available methods, the modification of starch surface by admicellar polymerization, to the best of our knowledge, has never been reported.

Admicellar polymerization was initially introduced by Wu *et al.*[16] It offers several advantages over traditional techniques. Accomplished in aqueous solution, this environmentally friendly technique can form nanoscale polymeric thin films, with minimum chemical usage and without the use of organic solvents. Additionally, this benign technique is able to maintain basic properties of the original material. The technique consists of four main steps (Scheme 1): admicelle formation on the surface, monomer adsolubilization, polymerization of monomers dissolved in admicelles and surfactant removal to expose the formed polymer film.

The first step is the formation of admicelle which is a bilayer template of adsorbed ionic surfactants on an oppositely charged surface. In the second step, an organic monomer is adsolubilized into the hydrophobic interior of the admicelles. The formation of admicelles as well as the monomer adsolubilization were clearly described in details by Dickson *et al.*[17] and Kitiyanan *et al.*[18] During the third step, an initiator is added and the temperature is increased to initiate radical polymerization of monomers adsolubilized inside the admicelles to produce ultrathin film of polymer on the surface. For the last step,

the modified substrate is thoroughly washed to remove the surfactant (on the upper layer, in contact with the solution) to expose the hydrophobic surface of the formed polymeric film. Inside the formed film-surfactant-substrate hybrid, the surfactant (on the lower layer, adsorbed on the surface) acts as a compatibilizer between the substrate and the polymer film, with a lower layer of head groups bonding with the hydrophilic substrate via ionic interactions and its tail groups bonding with the hydrophobic polymer film via hydrophobic interactions.[19] Thereby, at the end of the process, the surfactant on the upper layer is removed during washing, whereas the surfactant on the lower layer stays in the middle, linking the substrate surface and the newly formed ultrathin polymeric film.

Applications of admicellar polymerization are numerous, from reinforcements of composites to value addition of functional textiles, as described by Ulman and Shukla in their review for the application of admicellar polymerization in the field of textiles.[20] Several researchers have applied admicellar polymerization to induce surface modification to make two components of their polymeric composites more compatible. Admicellar polymerization was successfully used to coat PMMA films on the surface of graphene nanosheets to enhance interfacial adhesion between PMMA-functionalized graphene nanoparticles and PLA matrix.[21] The technique was also effectively applied to coat PMMA on the surface of sisal fiber to improve the compatibility between the sisal fiber and the surrounding polymeric matrix in a composite.[22] Pongprayoon *et al.*[23] also successfully applied admicellar polymerization to coat a thin film of polystyrene on cotton. Radiation-induced admicellar polymerization was utilized to coat polyisoprene on silica surface to improve the compatibility between modified silica and rubber.[24] The results revealed that mechanical properties of rubber reinforced with the modified silica were superior to those reinforced with unmodified silica. Examples from these studies emphasized the advantages of using admicellar polymerization as an effective method to enhance compatibility between a filler and a polymer matrix, which ultimately leads to improved mechanical properties of their composites. Moreover, a study by Nontasorn *et al.*[25] proved that the application of admicellar polymerization for surface modification can be scaled up from a batch reactor to a continuous stirred-tank reactor to provide a consistent product. Therefore, the surface modification of starch by this technique and its blend with PLA has high potential to be practical for industrial applications as well.

The objective of this research is to apply admicellar polymerization to improve compatibility between PLA and CS by coating ultrathin film of PMMA on the surface of CS. PMMA was chosen for this work simply due to excellent compatibility between PMMA and PLA[21] which is attributed to the interaction of ester groups present in both PMMA and PLA as well as their similar hydrophobicity. The increased hydrophobicity of PMMA modified cassava starch was verified by contact angle measurement. The formation of PMMA film on the surface of starch was confirmed by iodine test, FTIR, TGA, XPS, and SEM. Results from mechanical properties were used to demonstrate that starch modified with PMMA by admicellar polymerization was more hydrophobic as well as more compatible with PLA than unmodified starch.

## EXPERIMENTAL

### Materials

PLA 2002D was purchased from Nature Works® (USA). Cassava starch (97.5% minimum dried basis, 17 − 20% solubility in hot water, ≤13% loss on drying, 0.11% ash, 0.04% insoluble ash, pH 6.23) was supplied by Bangkok Inter Food Co. Ltd. (Thailand). Methyl methacrylate (MMA) (99%) was procured from Aldrich (Netherlands). Poly(methyl methacrylate) (PMMA, broad molecular weight standard, $M_w = 96{,}700$, $M_n = 44{,}700$) was bought from Aldrich (USA). Cetyltrimethylammonium bromide (CTAB) (98%) was obtained from Amresco (Germany). Ammonium persulphate (98%) was acquired from Ajax Finechem Pty. Ltd. (New Zealand). Acetone (95%) was supplied by Merck (Germany). Ethanol (95%) was procured from Fisher Scientific (USA). All chemicals were used as received.

### Admicellar Polymerization of MMA on CS

2.8 g (0.0075 mol) of CTAB was dissolved in 1000 ml of distilled water. 1 g of CS was mixed with 50 mL of CTAB solution. The mixture was stirred for 24 h. Then, 0.94 mL of ethanol and MMA (1.197, 1.595, and 1.995 mL) were added. The molar ratio of surfactant to monomer (CTAB:MMA) was varied (1:30, 1:40, and 1:50) to determine the optimum condition. The mixture was then stirred for another 24 h. Then, 0.017 g of ammonium persulphate was added into the mixture and the temperature was raised to and kept at 30 °C for 48 h to induce the admicellar polymerization. The mixture was subsequently filtered and washed several times with distilled water until the unnecessary surfactant was completely removed. The obtained modified starch (MS) was later dried in an air oven at 60 °C for 24 h.

### Film Formation Analysis and Surface Behavior of MS

PMMA film coated on CS after admicellar polymerization was analyzed and compared using two methods, solvent extraction and thermal gravimetric analysis. For solvent extraction method, the admicellar-treated cassava starch was extracted by acetone at room temperature for 24 h. The amount of PMMA coating on starch surface was calculated from the weight loss using the following equation:

$$\%\ \text{Weight loss} = (W_b - W_a) \times 100 / W_a$$

where $W_b$ is the weight before extraction and $W_a$ is the weight after extraction. Solvent extraction of CS over 24 h in acetone was also performed, as a control experiment. The add-on weight to the PMMA-coated starch after admicellar polymerization was determined using thermal gravimetric analysis. A thermogravimetric analyzer from Mettler Toledo (TGA, SDTA851$^e$) was used for thermogravimetric analysis. A heating rate of 10 °C/min from ambient temperature to 800 °C was applied. Thermal degradation experiments were done under nitrogen purge. The flow rate used for all experiments was 90 mL/min.

The surface behavior of CS and MS was analyzed by a contact angle measurement to compare their hydrophobicity. Contact angle measurement was performed using film samples of CS and MS. Water contact angles of samples were measured using a Krüss DSA100 contact angle goniometer (Krüss GmbH,

**Table I.** Sample Abbreviated Names and Formulation of PLA-TPS Blends

| Sample Name | PLA:TPS (w/w) | PLA (g) | CS (g) | MS (g) | Glycerol (g) |
|---|---|---|---|---|---|
| PLA | 100:0 | 100 | – | – | – |
| CS10 | 90:10 | 90 | 7 | – | 3 |
| CS20 | 80:20 | 80 | 14 | – | 6 |
| CS30 | 70:30 | 70 | 21 | – | 9 |
| MS10 | 90:10 | 90 | – | 7 | 3 |
| MS20 | 80:20 | 80 | – | 14 | 6 |
| MS30 | 70:30 | 70 | – | 21 | 9 |

Germany) at ambient temperature. Contact angle was evaluated using static drop method. Drop volumes of de-ionized water were 10 μL and the average contact angle value was obtained by measuring the same sample at three different positions.

### Characterization of MS

PMMA ultrathin film formed on CS surface was characterized by iodine test, FTIR, XPS, and SEM. For iodine test, CS and MS powders were simply dispersed in distilled water and iodine solution was dropped into the mixture to observe coloration. Chemical characterization of CS, MS and PMMA was done using a Tensor 27 Fourier transform infrared spectrometer (Bruker, Germany). Sixteen co-added scans were collected with a resolution of 4 $cm^{-1}$ in attenuated total reflection (ATR) mode. XPS measurements were made on a Thermo Scientific K-Alpha spectrometer (USA) with a mono chromatized Al Kα X-ray source (1486.6 eV photons) at a constant dwell time of 100 ms for several scans and pass energy of 30 eV with step of 0.1 eV for region scan spectra and 200 eV with step 1 eV for survey scan spectra. The pressure in the analysis chamber was maintained at $2.67 \times 10^{-7}$ pascal or lower. Processing of the data was carried out by the Avantage software. A scanning electron microscope (SEM) by JEOL (Model JSM-5410LV) equipped with an accelerated voltage of 20 kV was used to study the morphology of CS and MS. Before the experiments, all samples were subjected to gold sputter coating under vacuum. For cross-sectional SEM analysis, the samples were freeze fractured in liquid nitrogen before being sputter-coated with gold.

### Preparation of PLA-CS And PLA-MS Blends

Before blending with PLA, CS, and MS were changed into thermoplastic starch (TPS) first. To prepare TPS, CS or MS was mixed with glycerol, at a weight ratio of 70:30, using a high speed mixer from Lab Tech Engineering Company Ltd. (Thailand) at 3000 rpm/min for 10 min. PLA pellets were dried in a vacuum oven at 75 °C for 24 h. A co-current twin-screw extruder LTE16-40 from Lab Tech Engineering Company Ltd. (Thailand) was used to mix PLA with TPS at three different weight ratios, as shown in Table I. Equipped with segmented screw of diameters of 16 mm and length per diameter (*L/D*) ratio of 40:1, the twin-screw extruder contains 10 barrel sections, with each section being 4D in length. The extruder screw speed was set at 50 rpm. For PLA, the temperatures of barrel heating zone I – XI and the die of the extruder were set to 155, 160, 170, 180, 180, 190, 190, 200, 200, and 190 °C, respectively. For PLA-CS and PLA-MS blends, these temperatures were set to 145, 160, 170, 180, 190, 200, 190, 180, 170, and 160 °C, correspondingly. At the die, the flow rate for PLA was about 13 g/min, while that of PLA-CS and PLA-MS blends was roughly 7 g/min. The extruded PLA-TPS pellets were later compressed by a compression molder from Lab Tech Engineering Company Ltd. (Thailand) to form 150 mm × 150 mm × 0.2 mm films. The pellets were pre-pressed and full-pressed at 170 °C for 10 and 2 min, respectively, followed by cold-pressing at room temperature for 2 min. The obtained blends were cut into dumbbell-shaped films. The blend samples were kept in zip-lock bags which were stored in a container containing the blue silica gel beads.

### Mechanical Properties

The mechanical properties were measured at room temperature on a tensile tester (AG-100kNG, Shimadzu, Japan) at a cross-head speed of 10 mm/min. Sample preparation was done using a SD-type lever-controlled sample cutter (SDL-100, Dumbbell Co., Ltd., Japan) and a super dumbbell cutter (SDMK-1000-D, Dumbbell Co., Ltd., Japan), according to the ASTMD-638-IV. For each blend composition at each condition, ten samples were tested and the results were averaged.

## RESULTS AND DISCUSSION

For selection of surfactant type for the admicellar polymerization of starch, the net charge on the surface of starch will determine whether a cationic or an anionic surfactant is suitable.[18,22] The pH at which the net charge on the surface is zero is called the point of zero charge (PZC). The zeta potential and PZC measurements were used for the surface study of starch. By measuring the zeta potential as a function of the pH, the PZC can be determined. 1g of cassava starch was added to 1L of water. The solution pH was adjusted from 1 – 10 using either HCl or NaOH. The zeta potential was measured using a Zetasizer. The zeta potential and PZC of cassava starch are shown in Figure 1.

It can be seen from Figure 1 that, in the neutral aqueous solution (pH 7), the zeta potential of starch was −13 mV. Figure 1 also shows that PZC for starch is 1.8. This means that at pH

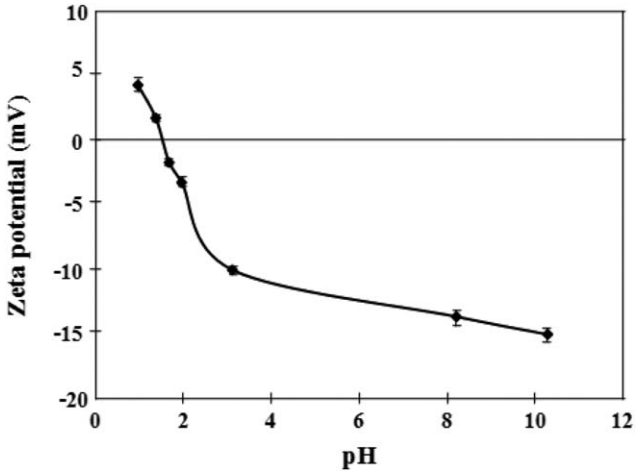


**Figure 1.** The zeta potential and PZC of cassava starch.

**Table II.** Film formation Analysis for CS and MS Samples by Solvent Extraction

| Sample | Film formation (%) |
|---|---|
| CS | 5.1 |
| MS prepared from CTAB:MMA = 1:30 | 7.4 |
| MS prepared from CTAB:MMA = 1:40 | 20.8 |
| MS prepared from CTAB:MMA = 1:50 | 22.2 |

below 1.8, the starch surface will be protonated and positively charged. In contrast, at pH above 1.8, starch will be negatively charged. As a result, when the pH of the aqueous solution is greater than 1.8, a cationic surfactant should be used because it will be well adsorbed on the negatively charged starch.[18,22] Therefore, cetyltrimethylammonium bromide (CTAB) was chosen as the cationic surfactant for this study.

**Film Formation Analysis and Surface Behavior of MS**

To determine the amount of PMMA film formed on starch surface, the weight loss of MS samples by solvent extraction was analyzed. Results for film formation analysis from extraction in acetone over 24 of MS samples, prepared at varied CTAB:MMA ratio, are shown in Table II, along with that of CS. The results revealed that for MS samples, film formation of PMMA increased as the ratio of surfactant to monomer was varied from 1:30 to 1:50. PMMA film formation seemed to reach saturation at CTAB:MMA ratio of 1:40. Hence this was determined to be the optimum condition for scale-up preparation of MS.

During monomer adsolubilization process, the monomer equilibrates between three phases: (1) inside the hydrophobic regions of the admicelles (2) in the aqueous phase of the supernatant and (3) in vapor phase inside the reaction container above the aqueous phase. Due to its organic nature, the monomer tends to stay inside the admicelles. However, the monomer can also easily evaporate into gas phase. Consequently, the monomer's equilibrium in the admicelles depends on the amount of surfactant, the volume of aqueous phase as well as the volume of empty space above the aqueous phase. The monomer was intentionally added to starch in excessive amount to make sure that there was enough monomer adsorbed inside the admicelles, during its equilibrium between these three phases, to undergo radical polymerization and form ultrathin film of PMMA on starch surface. The surplus monomer, free PMMA as well as the outer layer of surfactant will be completely removed during subsequent filtration and several times of washing.

TGA was also used to determine the amount of PMMA film formed on starch surface for MS sample synthesized at the optimum condition. The TGA and dTGA thermograms of CS, MS as well as standard PMMA are displayed in Figure 2. The original TGA thermograms are shown in a small inset at the top right corner, while the new TGA thermograms (after the normalization due to difference in moisture content) are displayed in the main figure. TGA thermogram of PMMA displays a one-stage weight loss process. Its dTGA thermogram shows that the onset of degradation was about 300 °C. The rate of weight loss reached a maximum at about 390 °C. Unlike PMMA, CS showed a well-separated two-stage weight loss process. The first degradation step at around 100 °C was due to moisture, resulting in 11.4% weight loss. The onset of the second major decomposition step was around 280 °C, with the maximum rate of weight loss at 320 °C. MS displayed similar thermal decomposition pattern. Its first degradation was also observed at about 100 °C, leading to 5.9% weight loss. The second one also started at 280 °C, with maximum rate of weight loss at around 320 °C.

Despite their similar thermal degradation pattern, a closer look at their TGA and dTGA thermograms revealed key distinctions that differentiate MS from CS. From the TGA thermograms, the first degradation step of CS and MS resulted in 11.4 and 5.9% weight loss, respectively. As previously mentioned, this early weight loss was due to moisture. Therefore, the difference in weight loss in this process implied the difference in moisture content in CS and MS. The weight difference between CS and MS due to moisture loss during the first degradation step was 5.5%. These TGA thermograms indicated that MS has low moisture content than CS. These results thus corresponded very well to the fact that PMMA coated on starch surface makes MS more hydrophobic, hence resulting in less moisture content than CS whose hydroxyl groups is rather hydrophilic.

Furthermore, TGA thermograms also revealed that after the major thermal decomposition of starch at 320 °C as well as

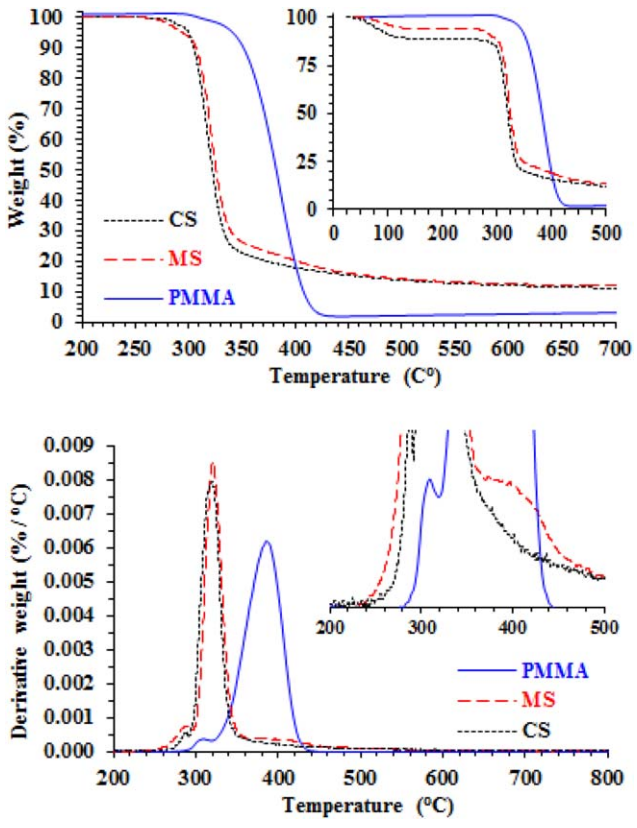


**Figure 2.** TGA and dTGA thermograms of CS, MS, and PMMA. [Color figure can be viewed in the online issue, which is available at wileyonlinelibrary.com.]

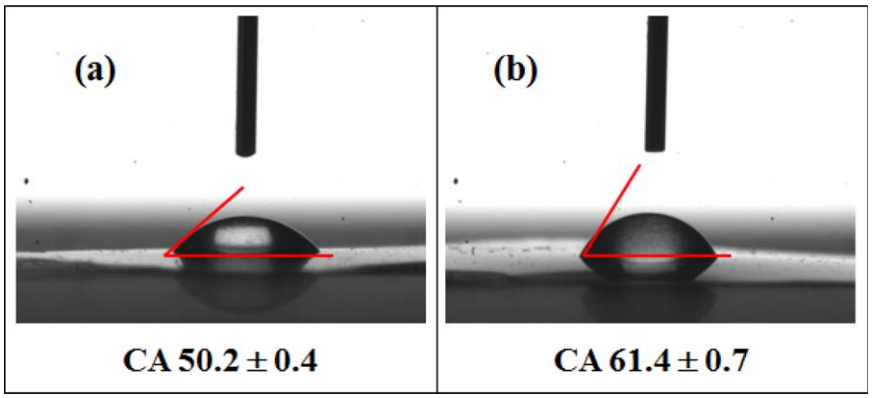


**Figure 3.** Contact angle measurement of CS (a) and MS (b). [Color figure can be viewed in the online issue, which is available at wileyonlinelibrary.com.]

before the major decomposition of PMMA at 400 °C, the remaining weight of MS was higher than that of CS. Consequently, the difference in the remaining weight, after starch finished its thermal degradation and before PMMA started its thermal decomposition, implied the add-on weight of PMMA film after admicellar polymerization. At 340 °C, the temperature at half way between the end of starch decomposition and the beginning of PMMA degradation, the remaining weight of CS and MS was 22.16 and 27.91%, respectively. The difference in their remaining weight was 5.75%.

However, the add-on weight cannot be directly calculated from the difference in remaining weight of the original TGA thermograms of CS and MS, due to the difference in moisture content in their original weight. To determine the correct add-on weight, the TGA thermograms of both CS and MS were normalized to the remaining weight after the first degradation was complete (i.e., 200 °C) to compensate for the difference in moisture content in CS and MS. The new TGA thermograms of CS and MS after the normalization are shown in the main figure. From these normalized TGA thermograms, at 340 °C, the remaining weight of CS and MS was 25.01 and 29.65%, respectively. These results suggested that the add-on weight of PMMA film, after radical polymerization of MMA monomer on starch surface, was about 4.64%. These results were similar to those reported by Yooprasert *et al.*[26] They investigated the admicellar polymerization of isoprene on silica, using three different surfactants, including CTAB. They also found out that the film formation of polyisoprene on silica surface (as determined by burning) was about 15% and weight loss (as determined by TGA) was around 6% for CTAB. The difference in film formation analysis as determined by solvent extraction and TGA stems from the fact that solvent extraction is less specific as the solvent used may be able to dissolve other compounds.[22] This is quite obvious from the film formation analysis, where acetone extraction resulted in 5.1% for CS and 20.8% for MS. In contrast, TGA is more specific since each polymer has its own unique degradation pattern. In this case, starch decomposes with maximum rate of weight loss at about 320 °C, whereas PMMA degrades with highest rate of weight loss at roughly 390 °C.[27,28]

As for the dTGA thermogram, MS revealed its additional degradation step centered at about 400 °C, as can be seen in a small close-up graph at the top right corner of the dTGA thermograms. This degradation step was absent in the dTGA thermogram of CS, but it clearly matched the major thermal decomposition of PMMA. These TGA results hence positively confirmed the presence of PMMA in MS.

After the scale-up preparation of MS, the hydrophobic behavior of CS and MS was investigated by a contact angle measurement. The results are shown in Figure 3. The contact angle measurement was performed to verify the improved hydrophobicity of MS induced by admicellar polymerization. CS and MS were casted into film samples. The contact angle of CS was determined to be 50.2 ± 0.4°, while that of MS was 61.4 ± 0.7°. The increased contact angle of MS, compared with CS, implied the presence of hydrophobic group on starch surface. Once again, these results substantiated the fact that MS was more hydrophobic than CS, thus confirming the formation of PMMA film on starch surface.

### Characterization of MS

Iodine test is one of the most well-known methods for starch characterization. Iodine dissolved in an aqueous solution reacts with starch, forming a characteristic purple-black color, which can be detected visually. This method was applied to characterize CS and MS. The samples were simply dispersed in distilled

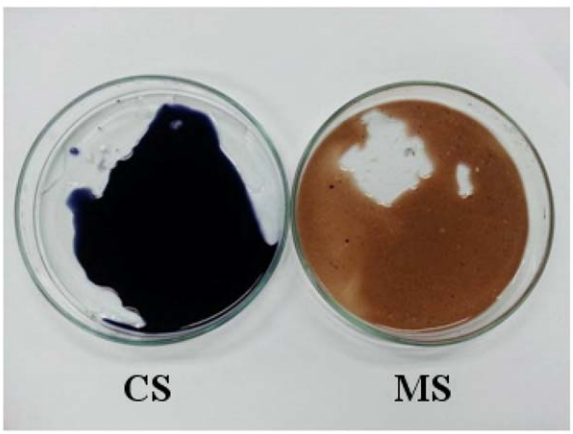


**Figure 4.** Iodine test for CS and MS. [Color figure can be viewed in the online issue, which is available at wileyonlinelibrary.com.]

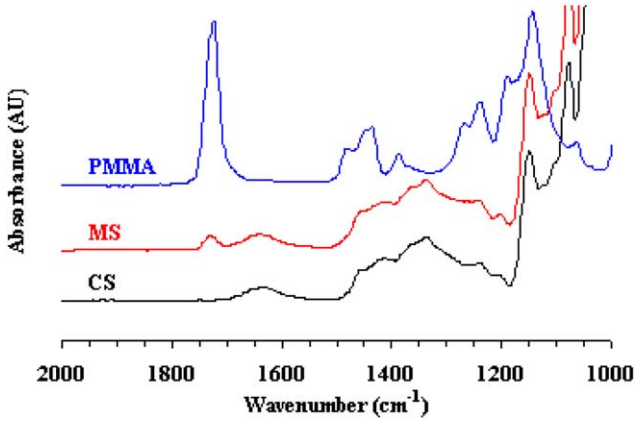


**Figure 5.** FTIR spectra of CS, MS, and PMMA. [Color figure can be viewed in the online issue, which is available at wileyonlinelibrary.com.]

water and iodine solution was dropped into the mixture for color observation. The results are demonstrated in Figure 4. Once mixed with iodine solution, CS solution instantly turned into purple-black color. Quite the opposite, MS displayed no changes in color, remaining light brown which is the original color of the iodine solution. This simple yet effective test, once more, clearly confirmed the change in surface behavior of MS.

To substantiate the achievement of surface modification of starch by admicellar polymerization, chemical characterization was performed using FTIR. FTIR spectra of CS and MS are shown in Figure 5, along with that of standard PMMA. FTIR spectrum of MS shows similar peaks commonly found in FTIR spectrum of CS.[29] Nevertheless, an additional peak at 1720 $cm^{-1}$ was found in the spectrum of MS. This peak corresponds to C═O stretching in ester,[30] which is one of the functional groups found in the chemical structure of PMMA, hence explaining the strong peak at 1720 $cm^{-1}$ in the spectrum of the standard PMMA. For that reason, the presence of this characteristic peak in the spectrum of MS distinctly validated the existence of PMMA in MS.

The surface chemical compositions of CS and MS were analyzed by XPS. Deconvolution of C 1s and O 1s peaks of both CS and MS samples are displayed in Figure 6. The peaks at roughly 286 and 532 eV are assigned to carbon and oxygen, respectively. Different binding energies of these C 1s and O 1s peaks are summarized in Table III.[31,32] For CS and MS, the C 1s signal showed four peaks at ~284.8, 286.4, 287.2, and 288.9 eV corresponding to C—C and/or C—H, C—O, O—CO and/or C═O and O—C═O, respectively. The first three functional groups are obviously present in the chemical structure of starch; however the last one is not. A tiny peak of O—C—O found in the C 1s deconvoluted XPS spectrum of CS sample is possibly due to the existence of small amount of lipids on the surface of starch.[31] This O—C═O peak was also found in the spectrum of MS sample, nevertheless their relative compositions were different. The increase in O—C═O peak in MS is most likely due to the presence of ester group found in the chemical structure of PMMA. CS and MS also showed different relative percentages of C—C/

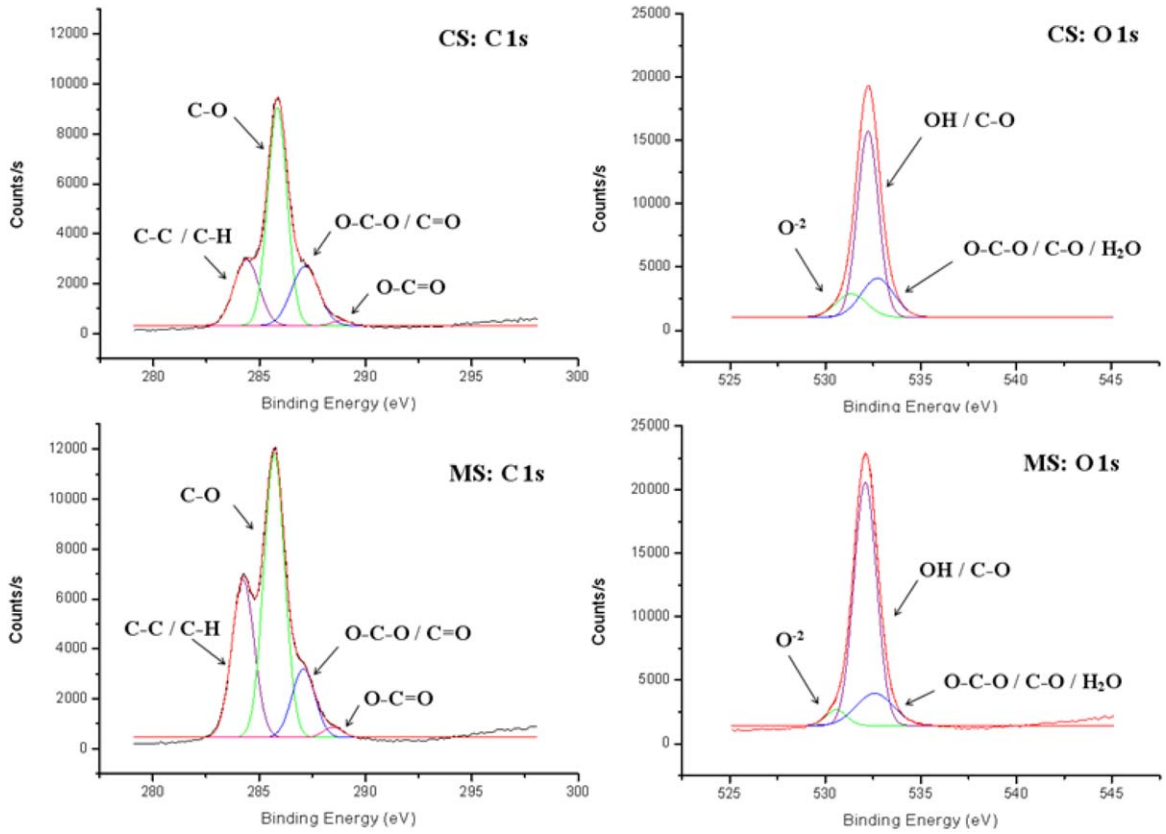


**Figure 6.** The high-resolution C 1s and O 1s deconvoluted XPS spectra of CS and MS. [Color figure can be viewed in the online issue, which is available at wileyonlinelibrary.com.]

**Table III.** Binding Energy of Different Functional Groups in C 1s and O 1s Peaks

| C 1s | C—C/ C—H | C—O | O—C—O/ C=O | O—C=O |
|---|---|---|---|---|
| Binding energy (eV) | 284.8 | 286.4 | 287.2 | 288.9 |
| O 1s | $O^{-2}$ | OH/C—O | O—C—O/ C—O/$H_2O$ | |
| Binding energy (eV) | 530.5 | 532.1 | 532.8 | |

C—H peak. The higher relative percentage of C—C/C—H peak in MS, compared to CS, is attributable to the presence of —C—$CH_2$— group in the chemical structure of PMMA as well as —$CH_2$—$CH_2$— group which is quite abundant in the chemical structure of CTAB on the surface of MS.

SEM was used to compare the surface morphology of CS and MS. Figure 7 displays the SEM micrographs of CS and MS, both at low magnification (500×) as well as high magnification (3,500×). The SEM micrographs at low magnification show that CS and MS particles are similar in size and shape, but plainly different in surface morphology. The difference in their surface morphology is more obvious at higher magnification. At 3,500× magnification, CS particles show a relatively smooth surface, whereas MS particles display comparatively rough exterior. The roughness is quite visible in each MS particle. The differences in surface morphology of CS and MS, once more, implied the success of surface modification of starch by admicellar polymerization.

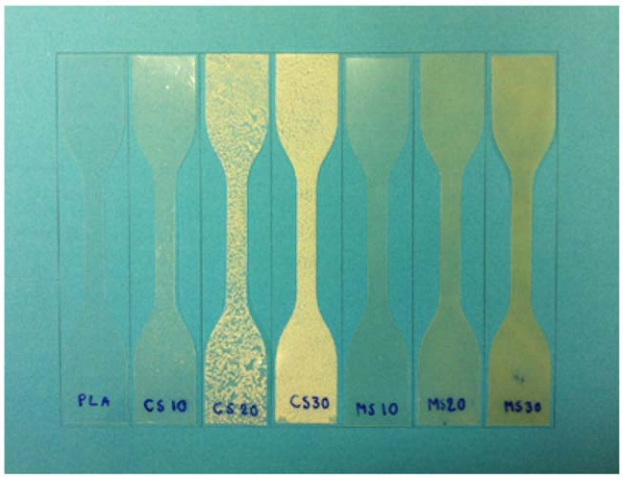


**Figure 8.** Physical appearance of pure PLA, PLA-CS and PLA-MS blends. [Color figure can be viewed in the online issue, which is available at wileyonlinelibrary.com.]

### Mechanical Properties of PLA-CS And PLA-MS Blends

After blending PLA and TPS prepared from CS and MS, physical appearances of PLA-CS and PLA-MS blends were compared, along with that of pure PLA sample, and the results are displayed in Figure 8. Pure PLA sample was quite clear and transparent. In contrast, PLA-CS blends were relatively opaque. Moreover, phase separation of starch particles from PLA matrix was rather obvious and increased with increasing content of TPS. Several research groups[7,33–35] also reported similar phase separation between PLA and starch, due to their incompatibility. As for

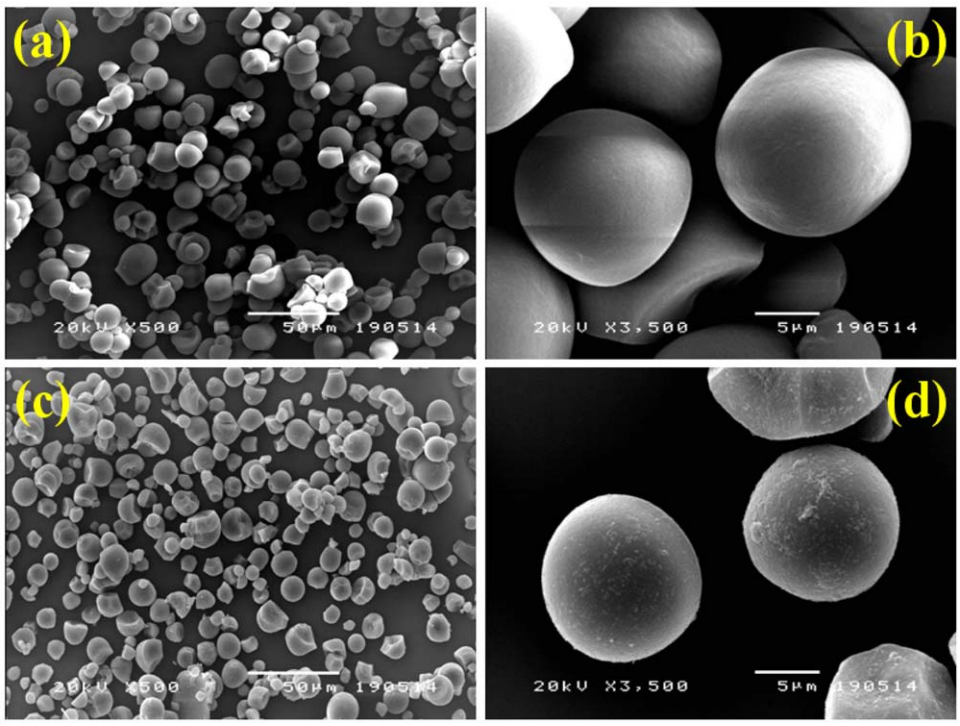


**Figure 7.** SEM micrographs of CS at magnification 500× (a) and 3,500× (b) and MS at magnification 500× (c) and 3,500× (d). [Color figure can be viewed in the online issue, which is available at wileyonlinelibrary.com.]

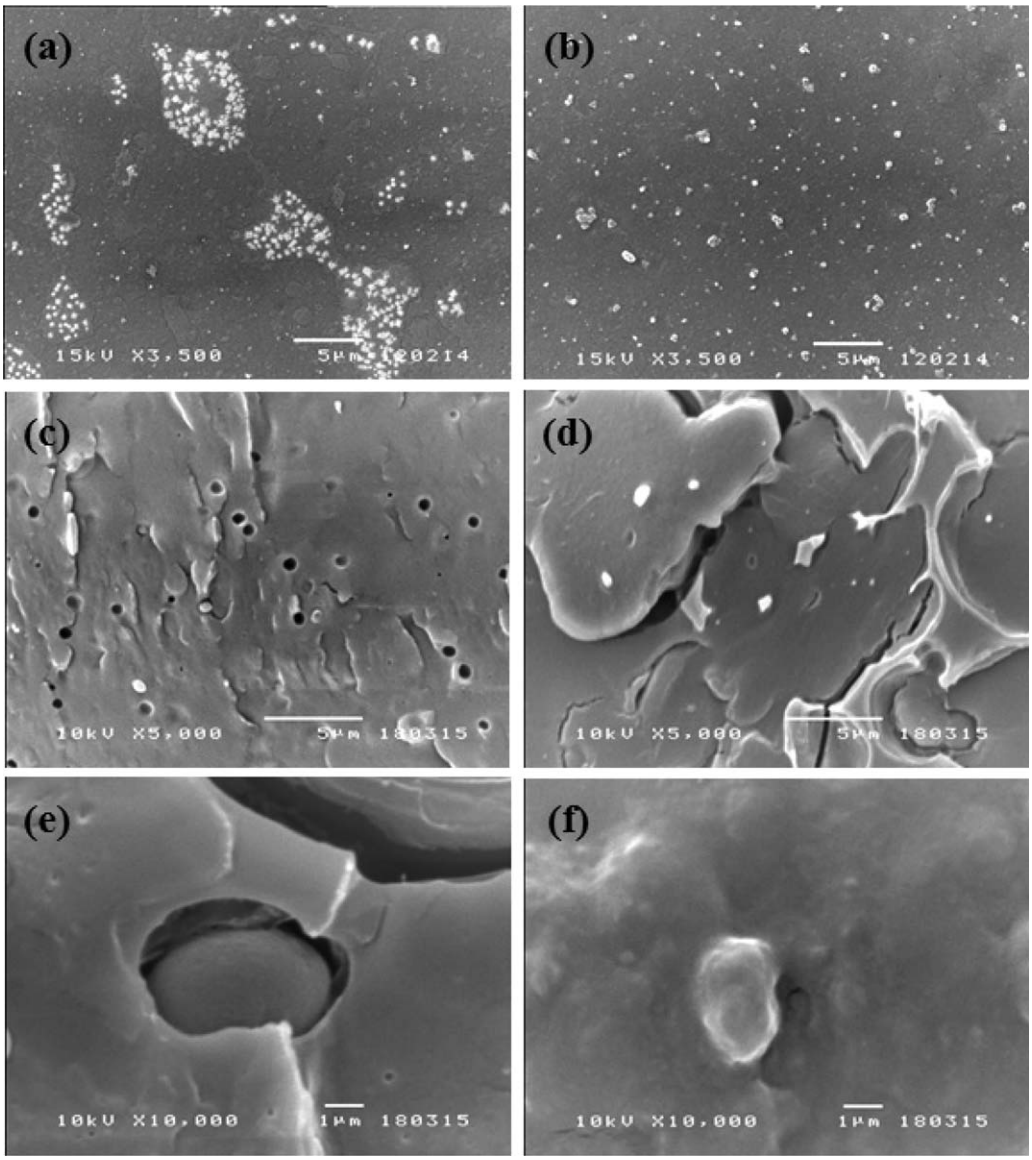


**Figure 9.** SEM results for surface morphology of CS30 (a) and MS30 (b).

PLA-MS blends, the samples were not as transparent as the neat PLA sample and their opaqueness also increased with increasing content of TPS. Nevertheless, they did not show obvious phase separation of starch particles in PLA matrix as clearly seen in PLA-CS blends. These results simply reflected the achievement of surface modification of starch in MS as well as the enhanced compatibility between PLA and MS.

SEM was used to compare both the surface and cross-sectional morphology of PLA-CS and PLA-MS blends. SEM results of CS30 and MS30 samples are displayed in Figure 9. For surface morphology, Figure 9(a,b) display distribution of CS and MS inside PLA matrix, respectively. Starch particles in CS30 sample obviously coalesced into agglomerates, resulting in poor dispersion. This is simply due to the fact that the surface of starch is full of hydroxyl groups. Distributing in a hydrophobic matrix, these hydrophilic groups tend to have strong interactions, thus resulting in agglomerates. Unlike CS30 sample, MS30 sample displays less agglomeration, offering much better dispersion. This stems from the fact that the surface of MS is coated with PMMA which is rich in ester groups. These ester groups are less hydrophilic and more compatible with the surface of PLA, thus leading to less agglomeration, better distribution as well as improved compatibility between PLA and starch particles in MS30 sample

For the analysis of the adhesion between the interfaces of starch and PLA, cross-sectional SEM images of CS30 and MS30 samples fractured in liquid nitrogen are shown at magnification 5,000× in Figure 9(c,d) and at magnification 10,000× in Figure 9(e,f), respectively. In Figure 9(c), the fracture morphology of CS30 shows many empty pores with free starch particles. The removal of these starch particles from the pores is most likely due to poor interfacial adhesion between PLA and starch. The cross-sectional morphology of CS30 sample at higher magnification, in Figure 9(e), displays that there is a cavity between the

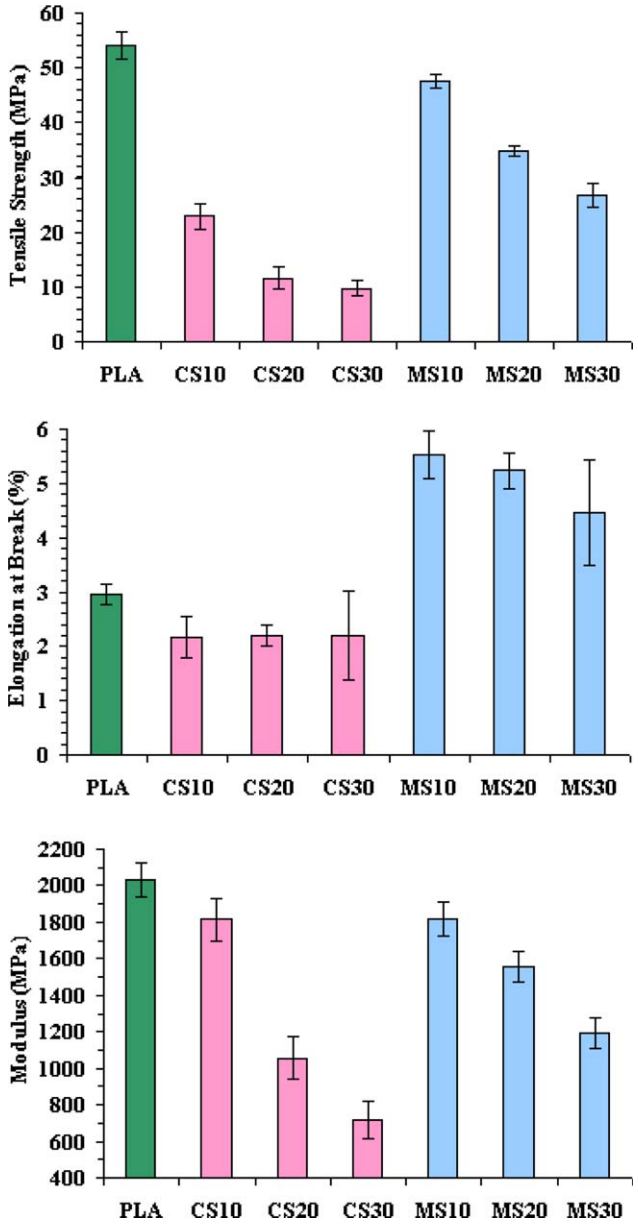


**Figure 10.** Mechanical properties of pure PLA, PLA-CS, and PLA-MS blends. [Color figure can be viewed in the online issue, which is available at wileyonlinelibrary.com.]

surface of PLA and starch particle. In contrast, in Figure 9(d), the fracture surface of MS30 shows several starch particles fixed within PLA matrix. The cross-sectional SEM image of MS30 sample at higher magnification, in Figure 9(f), also shows that there is no void between the surface of starch particle and PLA matrix. The fact that starch particles in MS samples are fixed within PLA matrix once more proves that the starch surface is coated with PMMA film. For this reason, starch particles in MS samples are able to adhere to PLA much better than those in CS samples. Additionally, the fracture surfaces of CS30 and MS30 display distinctive features. Smooth fractures are observed in Figure 9(c), implying that CS30 is relatively brittle, thus getting detached neatly during fracture. In contrast, uneven fractures are seen in Figure 9(d), indicating that MS30 is more ductile, hence resulting in comparatively irregular fracture surface.[36]

To further confirm the improved compatibility between PLA and MS, the mechanical properties of PLA-CS and PLA-MS blends, in terms of tensile strength, elongation at break and modulus, were measured. Figure 10 reveals the effect of starch content on tensile strength, elongation at break and modulus for PLA-CS and PLA-MS blends. For PLA-CS blends, tensile strength of the blends decreased markedly from roughly 55 to 10 MPa, as the starch content increased from 0 to 30%. Elongation at break as well as modulus of PLA-CS blends also declined with starch content. The deterioration in mechanical properties of PLA-CS blends is simply due to poor compatibility between PLA and CS.

Tensile strength of PLA-MS blends also decreased with increasing TPS content. Nevertheless, unlike PLA-CS blends, PLA-MS blends did not show drastic decrease of mechanical properties, but rather displayed gradual decline. The tensile strength of PLA-CS blends at 10, 20, and 30% of TPS content was 22.87, 11.63, and 9.70 MPa, in that order, whereas that of PLA-MS blends was 46.85, 34.21, and 25.97 MPa, respectively. The percentage increase was ~105, 194, and 168, correspondingly. The modulus also displayed trends similar to those observed in tensile strength. In contrast, elongation at break data offered interesting results. The elongation at break of each PLA-MS blend was even higher than that of the neat PLA sample. This stems from the fact that PLA is generally brittle, while TPS is usually more flexible.[35] The improved compatibility between PLA and MS makes it possible for PLA matrix to transfer stress formed during mechanical tests to dispersed phase of MS, thus leading to higher elongation of the PLA-MS blends. These results, once again, positively authenticated improved compatibility between PLA and MS.

## CONCLUSIONS

Admicellar polymerization was successfully applied to coat the surface of starch with PMMA to render it more hydrophobic and more compatible with PLA. Results from contact angle measurement validated the increased hydrophobicity of PMMA modified cassava starch, while results from iodine test, FTIR, TGA, XPS, and SEM clearly confirmed the formation of PMMA film on the surface of starch. Improvements in tensile strength and elongation at break substantiated the fact that starch modified with PMMA by admicellar polymerization was more hydrophobic as well as more compatible with PLA than unmodified starch. The present work thus demonstrates that the improved compatibility between PLA and starch can be induced by the modification of starch surface through admicellar polymerization.

## ACKNOWLEDGMENTS

The authors gratefully acknowledge financial support from Coordinated Research Project (CRP Contract number 16403) granted by the International Atomic Energy Agency (IAEA).

## REFERENCES


1. Ray, S. S. *Acc. Chem. Res.* **2012**, *45*, 1710.
2. Vink, E. T. H.; Rabago, K. R.; Glassner, D. A. *Polym. Degrad. Stabil.* **2003**, *80*, 403.
3. Rasal, R. M.; Janorkar, A. V.; Hirt, D. E. *Prog. Polym. Sci.* **2010**, *35*, 338.
4. Teixeira, E. M.; Da Roz, A. L.; Carvalho, A. J. F.; Curvelo, A. A. S. *Carbohyd. Polym.* **2007**, *69*, 619.
5. Lopez, O. V.; Ninago, M. D.; Soledad Lencina, M. M.; Garcia, M. A.; Andreucetti, N. A.; Ciolino, A. E.; Villar, M. A. *Carbohydr. Polym.* **2015**, *126*, 83.
6. Shi, R.; Zhang, Z.; Lui, Q.; Han, Y.; Zhang, L.; Chen, D.; Tian, W. *Carbohydr. Polym.* **2007**, *69*, 748.
7. Yang, Y.; Tang, Z.; Ziong, Z.; Zhu, J. *Int. J. Biol. Macromol.* **2015**, *77*, 273.
8. Ke, T.; Sun, X. *Cereal Chem.* **2000**, *77*, 761.
9. Kim, S. H.; Chin, I.; Yoon, J.; Kim, S. H.; Jung, J. *Korea Polym. J.* **1998**, *6*.
10. Ren, J.; Liu, Z. C.; Ren, T. B. *Polym. Polym. Compos.* **2007**, *15*, 597.
11. Wang, N.; Yu, J.; Chang, P. R.; Ma, X. *Carbohydr. Polym.* **2008**, *71*, 109.
12. Huneault, M. A.; Li, H. *Polymer* **2007**, *48*, 270.
13. Ren, J.; Fu, H.; Ren, T.; Yuan, W. *Carbohydr. Polym.* **2009**, *77*, 576.
14. Wokadala, O. C.; Emmambux, N. M.; Ray, S. S. *Carbohydr. Polym.* **2014**, *112*, 216.
15. Jariyasakoolroj, P.; Chirachanchai, S. *Carbohydr. Polym.* **2014**, *106*, 255.
16. Wu, J.; Harwell, J. H.; O'Rear, E. A. *J. Phys. Chem.* **1987**, *91*, 623.
17. Dickson, J.; O'Haver, J. *Langmuir* **2002**, *18*, 9171.
18. Kitiyanan, B.; O'Haver, J. H.; Harwell, J. H.; Osuwan, S. *Langmuir* **1996**, *12*, 2162.
19. Rosen, M. J.; Kunjappu, J. T. In Surfactants and Interfacial Phenomena; 4th Ed.; Wiley: New Jersey, **2012**; Chapter 2, p 44.
20. Ulman, K. N.; Shukla, S. R. *Adv. Polym. Tech.* **2015**, *0*, 21556, 10.1002/adv.21556.
21. Lei, L.; Qiu, J.; Sakai, E. *Chem. Eng. J.* **2012**, *209*, 20.
22. Pongprayoon, T.; Yanumet, N.; Sanghong, S. *Colloids Surf* **2008** *A 320*, 130.
23. Pongprayoon, T.; Yanumet, N.; O'Rear, E. A.; Alvarez, W. E.; Resasco, D. E. *J. Colloid Interface Sci.* **2005**, *281*, 307.
24. Pongprayoon, T.; Yoopraset, N.; Suwanmala, P.; Hemvichian, K. *Rad. Phys. Chem.* **2012**, *81*, 541.
25. Nontasorn, P.; Chavadej, S.; Rangsunvigit, P.; O'Haver, J. H.; Chaisirimahamorakot, S.; Na-Ranong, N. *Chem. Eng. J.* **2005**, *108*, 213.
26. Yooprasert, N.; Pongprayoon, T.; Suwanmala, P.; Hemvichian, K.; Thumcharern, G. *Chem. Eng. J.* **2010**, *156*, 193.
27. Yoon, S.; Park, M.; Byun, H. *Carbohydr. Polym.* **2012**, *87*, 676.
28. Canche-Escamilla, G.; Canche-Canche, M.; Duarte-Aranda, S.; Caceres-Farfan, M.; Borges-Argaez, R. *Carbohydr. Polym.* **2011**, *86*, 1501.
29. Suwanmala, P.; Hemvichian, K.; Hoshina, H.; Srinuttrakul, W.; Seko, N. *Rad. Phys. Chem.* **2012**, *81*, 982.
30. Lambert, J. B.; Shurvell, H. F.; Lightner, D. A.; Graham Cooks, R. Organic Structural Spectroscopy; Prentice Hall: New Jersey, **1998**; Chapter 8.
31. Wei, B.; Xu, X.; Jin, Z.; Tian, Y. *PLoS ONE* **2014**, *9*, e86024. DOI: 10.1371/journal.pone.0086024.
32. Ochoa, N.; Bello, M.; Sancristobal, J.; Balsamo, V.; Albornoz, A.; Brito, J. L. *Mater. Res.* **2013**, *16*, 1209.
33. Suin, A. B. S.; Khatua, B. B. *Carbohydr. Polym.* **2014**, *110*, 430.
34. Ferreira, W. H.; Carmo, M. M. I. B.; Silva, A. L. N.; Andrade, C. T. *Carbohydr. Polym.* **2015**, *117*, 988.
35. Martin, O.; Averous, L. *Polymer* **2001**, *42*, 6209.
36. Qu, P.; Gao, Y.; Wu, G.; Zhang, L. *BioResources* **2010**, 1811, 5.

**SGML and CITI Use Only**
**DO NOT PRINT**